Proceedings of the 21st ICSMGE, Vienna, Austria, 14 – 19 June 2026. Pistrol, Adam & Schweiger (eds.)
Published by: ÖGG, Austrian Society for Geomechanics, Salzburg, Austria, ISBN 978-3-9503898-4-5
https://doi.org/10.53243/ICSMGE2026-1927

Nickel-Dependent Enhancement of Microbially Induced Calcite Precipitation for Bio-cementation of Coal Mine Overburden

Syamili Sarma
Indian Institute of Technology Guwahati, GUWAHATI, India, s.syamili@iitg.ac.in

Anil Kumar Mishra
Indian Institute of Technology Guwahati, GUWAHATI, India

ABSTRACT: Microbially induced calcium carbonate precipitation (MICP) represents a low-carbon, environmentally benign alternative for soil stabilisation and remediation of metal-contaminated matrices. This study examined the effect of Ni^{2+} on the precipitation potential of *Sporosarcina pasteurii* ATCC11859, with emphasis on its role as a structural cofactor in urease and fine-tuning the concentration of Ni^{2+} can improve the efficacy of the process. The grown bacterial cells are mixed with urea, calcium chloride, and graded Ni^{2+} concentrations to assess precipitation efficiency. The controlled laboratory experiments evaluated bacterial performance, revealing that low levels (0.01 mM) of Ni^{2+} enhanced the urease activity and calcite precipitation. This enhancement is attributed to Ni^{2+}'s role in stabilising the urease active site, thereby improving enzymatic efficiency. At moderate Ni^{2+} concentrations, *S. pasteurii* maintained moderate bio-cementation potential, despite the potential inhibitory effects of metal toxicity, demonstrating a notable degree of metal tolerance. Application of MICP to contaminated overburden soil resulted in an 11-fold increase in unconfined compressive strength within 5 days. These findings underscore the technology's potential for simultaneous mechanical improvement and effective management of Ni-contaminated matrices, positioning MICP as a viable cleaner production strategy for sustainable geotechnical applications.

KEYWORDS: Microbially Induced Calcite Precipitate, Nickel Toxicity, Sporosarcina pasteurii, Enzyme Activity.

1 INTRODUCTION

Microbially Induced Calcite Precipitation (MICP) has emerged as a transformative biotechnology, demonstrating rapid advancements and widespread applicability across various scientific and engineering disciplines (Fu et al., 2023). In recent years, innovative research on MICP has significantly enhanced both its fundamental understanding and practical applications, particularly within the domains of sustainability, geotechnical engineering, and materials science. The growing multidisciplinary interest in MICP is driven by its potential to address pressing environmental and engineering challenges while ensuring scalability, cost-effectiveness, and environmental compatibility (Carter et al., 2023). Within geotechnical engineering, MICP offers a promising, eco-friendly alternative to conventional methods of soil stabilisation, material improvement, heavy metal immobilisation, and industrial waste valorisation (Mi et al., 2023; Yin et al., 2023). Unlike traditional chemical stabilisation techniques that often rely on carbon-intensive binders such as cement or lime, MICP utilises microbial activity to induce calcite precipitation, thereby reducing greenhouse gas emissions and promoting cleaner production. This inherent sustainability has made MICP a focus of global research efforts, especially as industries seek to transition toward low-carbon, environmentally responsible solutions (Fouladi et al., 2023).

Despite the growing body of work on MICP, most geoenvironmental studies have predominantly emphasised application-oriented aspects, often overlooking the crucial microbiological factors that govern the process efficiency (Sarma et al., 2025). Given that MICP is inherently an interdisciplinary phenomenon, coupling microbiology, chemistry, and geotechnical engineering, a holistic approach is essential for optimising its performance. Equal emphasis on bacterial activity and geotechnical parameters is critical to enhance the overall effectiveness and reliability of MICP processes.

Heavy metal contamination, particularly in soils and groundwater, poses a severe environmental and public health challenge due to the toxicity and non-biodegradability of metals such as nickel (Ni^{2+}), cadmium, and lead (Cui et al., 2023). These contaminants are frequently introduced through anthropogenic activities, including mining, industrial effluents, and agricultural practices, and they can persist in ecosystems for decades. Even at trace levels, heavy metals can disrupt soil quality, impair crop productivity, and enter the food chain, causing bioaccumulation and health hazards for both humans and animals (Giannis et al., 2010). Among these contaminants, nickel pollution has become a critical concern due to its widespread industrial use and associated toxicological risks (El-Naggar et al., 2021). Interestingly, nickel also plays a dual role in biological systems. While elevated Ni^{2+} concentrations are toxic, trace amounts of this metal are essential as a cofactor for several enzymes, including urease, a key enzyme in the MICP process. Urease, a metalloenzyme, catalyses the hydrolysis of urea into carbonate and ammonium ions, which subsequently facilitate calcium carbonate precipitation (Ge et al., 2013). Given the catalytic dependence of urease on Ni^{2+}, fine-tuning Ni^{2+} concentrations can enhance the kinetics of urea hydrolysis and, consequently, the efficiency of the bio-cementation process.

This study focuses on exploring the role of Ni^{2+} concentration in enhancing the bio-cementation potential of the bacterial strain used in MICP. We systematically investigate the impact of varying Ni^{2+} dosages on the process efficiency, aiming to determine the optimal concentration that maximises calcite precipitation while minimising toxicity effects. The optimised Ni^{2+} dosage is further applied to soil stabilisation experiments, demonstrating its potential to enhance the mechanical strength and durability of treated soils. These findings not only advance the scientific understanding of metal–microbe interactions in MICP but also contribute to the development of scalable, sustainable solutions for geotechnical applications, heavy metal immobilisation, and industrial waste valorisation.

2 MATERIALS AND METHODS

2.1 *Bacterial Strain and Reagents*

The bacterial strain *Sporosarcina pasteurii* ATCC 11859, employed in this study, was procured from the American Type Culture Collection (ATCC). The lyophilised culture supplied in a sealed ampoule was reconstituted in Tris–ammonium sulphate (TAS) medium. The resulting suspension was transferred to fresh TAS medium and incubated under optimal conditions (30 °C, 180 rpm) to facilitate recovery and growth. Following initial propagation, single colonies were isolated on solid TAS medium to ensure purity. Glycerol stocks of the recovered strain were subsequently prepared and stored at −80 °C for long-term preservation and future experiments (Yang et al., 2024). To validate that the obtained strain has ureolytic activity, a qualitative assay using a phenol-red-based urease test was carried out with *E. coli* as the negative control, along with a blank phenol-red-based medium.

All the chemicals and reagents used for the study were obtained from Himedia Laboratories Private Limited, Industry Biotechnology, and Sisco Research Laboratories Private Limited.

2.2 *Soil*

Soil used in the study, hereafter referred to as OB, was collected from the North East Coal mine, India. The physical, chemical, and geotechnical properties of the soil were determined as per the ASTM standards, and X-ray Diffraction was carried out to find the mineralogical characteristics. The total metal concentration and leachability of the heavy metals were analysed as per the protocol of the Environmental Protection Agency (EPA, 1992).

2.3 *Growth Media (GM)*

The growth medium TAS comprises Tris Buffer-15.57 g, Ammonium Sulphate-10 g, Yeast extract-20 g and Urea-20 g in 1 L of media. Fermentation was performed in 250 mL Erlenmeyer flasks using a 2% (v/v) inoculum adjusted to an optical density (OD_{600nm}) of 1. At defined time intervals, 2 mL aliquots were withdrawn for analysis.

2.4 *Precipitation Media (PM)*

The PM comprised 0.5 M $CaCl_2$ and 0.5 M urea in a total volume of 50 mL and was used to evaluate the bio-cementation potential of the bacterial strain. An aliquot (1 mL) of fermentation broth, adjusted to an OD_{600nm} of 1, was centrifuged, and the cells were then washed three times with phosphate buffer solution (pH = 7). The washed cells were then introduced into the PM, and samples were collected at defined time intervals to quantify residual Ca^{2+} (Sarma et al., 2025). After the residual Ca^{2+} concentration in the PM was constant, the PM was filtered through Whatman No. 1 filter paper, and the precipitate was washed with sterile Milli-Q, oven-dried, and subjected to gravimetric analysis. To study the stimulatory effect of $NiCl_2$, the concentration was varied from 0 to 0.05 M in the PM during the bio-cementation potential experiments. As a control PM without inoculation of bacteria was used to check the abiotic precipitation

2.5 *Analytical methods*

2.5.1 *Biomass*

Biomass concentration was determined by centrifuging 1 mL of fermentation broth at 13,000 rpm for 5 min, washing the pellet with 0.9% NaCl, and measuring OD_{600nm} using a UV-VIS spectrophotometer (Varian 50 Bio; Milpitas, CA, USA).

2.5.2 *Enzyme Activity*

Urease activity was determined using the electrical conductivity (EC) method. Briefly, 1 mL of bacterial broth was mixed with 9 mL of 1.11 M urea, and the change in EC was monitored for 5 min at room temperature (25 ± 3 °C). The rate of change in EC (mS cm^{-1} min^{-1}) was used to calculate urease activity using equation 1, with correction for the dilution factor (Whiffin, 2004). A urea solution without bacterial broth served as the control.

$$Urea\ hydrolysed\ \left(\frac{mM}{Min}\right) = \frac{11.11 \times Change\ in\ conductivity\ \times dilution\ factor}{5} \quad (1)$$

2.5.3 *Calcium Concentration*

To determine the residual concentration of calcium in the PM, the samples collected at regular intervals were centrifuged at 13000 rpm for 5 minutes, and the supernatant was used. Flame photometry was used to determine the concentration of Ca^{2+} after diluting the supernatant (APHA, 1992).

2.6 *Unconfined Compressive Strength (UCS)*

Soil columns were constructed at the bulk density and field moisture content in cylindrical columns having a diameter of 3.8 cm and a height of 7.6 cm. Two-phase injection was used to introduce the treatment solution and bacteria to the soil system (Sarma et al., 2025). Initially, the bacterial solution was injected at a rate of 10 rpm, followed by the injection of optimised $NiCl_2$, along with 1M $CaCl_2$, 1 M urea and 1 mL of TAS medium. The sample was subjected to loading after 5, 7, 14, and 21 days of treatment to determine its strength. Figure 1 depicts the experimental setup for injecting the treatment solution into the soil system.

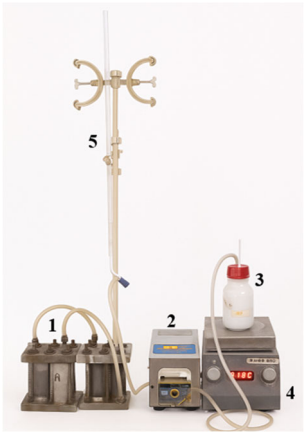

Figure 1. Experimental design for carrying out the MICP treatment.

3 RESULTS AND DISCUSSION

3.1 *Physical and Geotechnical Properties of OB*

The OB material exhibited a maximum dry density of 1.55 g cm^{-3} and an optimum moisture content of 15.7%, as determined by the Proctor compaction test. The in-situ field density was 1.20 g cm^{-3}, with a natural water content of 5%. Particle-size analysis (Fig. 2a) indicated a fines fraction of 22%. A free swell index of 2 mL per 2 mg confirmed the non-expansive character of the material, and Atterberg limit testing classified it as non-

plastic. In its untreated state, the OB sample yielded a mean unconfined compressive strength of 46.6 kPa. X-ray diffraction analysis (Fig. 7) revealed quartz (2θ = 26.6°) as the dominant mineral phase, accompanied by kaolinite, illite, alumina, hematite, feldspar, and minor accessory minerals.

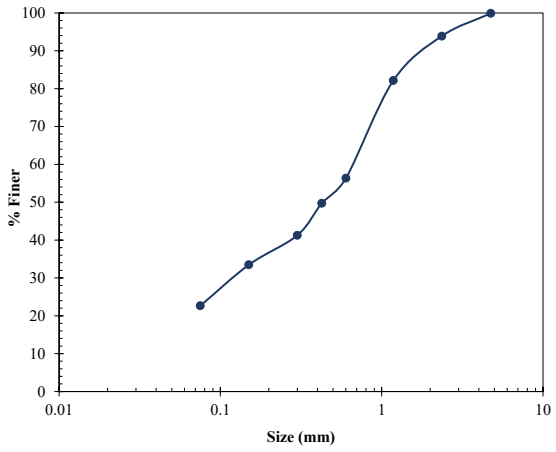

(a)

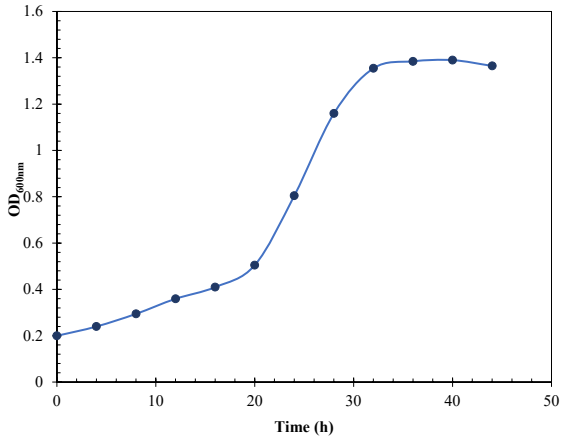

(b)

Figure 2. (a) Particle-size distribution curve of the OB sample. (b) Growth profile of *Sporosarcina pasteurii* ATCC 11859 in TAS medium.

3.2 *Growth curve of s. pasteurii*

The dynamic profile of *S. pasteurii* ATCC 11859 was typically an S-shaped growth curve (Fig. 2b), with a maximum OD_{600nm} of 1.6 ± 0.064 and entered the stationary phase after 32 h of inoculation in the TAS medium. The maximum enzyme activity was found to be 259.88 mMureahydrolyzed/h (Fig. 6). From the exponential phase, when OD_{600nm} was 1, the bacterial cells were harvested for further analysis (Yang et al., 2024).

The phenol red-based urease assay provided a clear qualitative distinction between the tested strains. *S. pasteurii* induced a pronounced pink colouration in the medium, whereas *E. coli* exhibited no perceptible colour change, confirming the ureolytic nature of the former. This response reflects the pH-dependent colour transition of phenol red, which shifts from yellow to pink as the medium becomes alkaline. The alkalinity arises from the enzymatic hydrolysis of urea by urease, producing ammonia and carbon dioxide, with the former increasing the pH. The observed result is consistent with the established biochemical role of urease in *S. pasteurii*, and its absence in E. coli. (Fig.3). No change was observed in the blank, indicating the absence of abiotic urea hydrolysis, and validating that the observed pH shift in the test samples resulted exclusively from microbial urease activity.

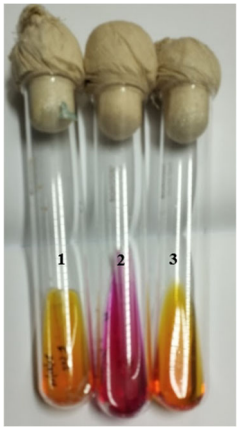

Figure 3. Qualitative Assay, 1- phenol-based medium with *E. coli*, 2-phenol-based medium with *S. pasteurii*, 3- blank phenol-based medium.

3.3 *Effect of Ni^{2+} concentration on the utilisation of Ca^{2+}*

For large-scale applications of MICP, enhancing system efficacy is essential from a sustainability perspective. As a metalloenzyme, urease requires Ni^{2+} as a critical cofactor for its activity (Ge et al., 2013). Determining the optimal Ni^{2+} concentration is therefore vital to achieving improved reaction kinetics.

The temporal profile of residual Ca^{2+} concentration in the PM, supplemented with varying concentrations of Ni^{2+} (0-50 mM), is shown in Fig. 3. In the PM without Ni^{2+}, *S. pasteurii* exhibited rapid Ca^{2+} depletion, with residual concentrations declining from 20 g/L to below 3 g/L within 8 h, indicative of efficient calcium carbonate precipitation.

In contrast, the presence of Ni^{2+} significantly altered Ca^{2+} consumption dynamics. At low Ni^{2+} levels (< 1 mM), the rate and extent of Ca^{2+} removal were marginally improved, with complete or near-complete depletion occurring within 4-6 h. In the case of PM with 0.01 mM Ni^{2+}, the complete depletion occurred at less than 6h. However, moderate concentrations ~ 10 mM caused a pronounced delay, with residual Ca^{2+} exceeding 1 g/L after 24 h of inoculation, suggesting partial inhibition of ureolytic activity and biomineralisation efficiency.

At the highest Ni^{2+} concentrations tested (20-50 mM), Ca^{2+} utilisation was severely suppressed, with residual concentrations remaining above 15 g/L even after 24 h. This strong inhibition is likely attributable to the toxic effect of Ni^{2+} ions on bacterial metabolism, including disruption of the enzymatic activity of urease. Similar inhibitory trends under heavy metal exposure have been reported in other ureolytic strains, where metal toxicity impedes cellular energy metabolism, enzyme folding, and membrane transport (Fopase et al., 2019; Rajasekar et al., 2025). No decrease in concentration of Ca^{2+} was observed in the sample without bacterial inoculation, eliminating the chance of abiotic precipitation.

The observed concentration-dependent inhibition underscores the importance of optimising heavy metal levels in cementitious biotreatment applications, particularly when processing industrial wastewaters or mine tailings with elevated Ni^{2+} content. Elevated Ni^{2+} levels compromise long-term microbial viability, reducing the sustainability of the process.

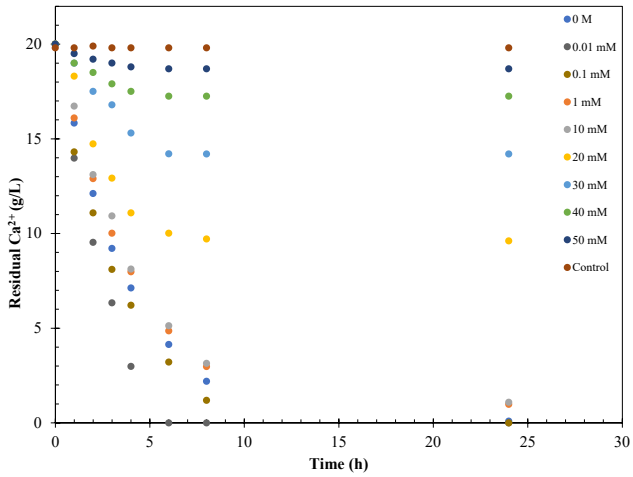

Figure 4. Residual Ca^{2+} concentration in the PM at different concentrations of Ni^{2+}.

3.4 *Effect of Ni^{2+} concentration on the precipitation potential*

The extent of calcium carbonate precipitation exhibited a clear dependence on Ni^{2+} concentration. In the PM without Ni^{2+}, *S. pasteurii* achieved a precipitation yield of ~2.16 g within 48 h of inoculation (Fig. 5).

At low Ni^{2+} concentrations (≤ 10 mM), precipitation efficiency remained high, with final yields comparable to the PM without Ni^{2+} and only a slight delay in reaching maximum precipitation (Fig.4). Apparently, a slight increase in the amount of precipitate was observed in the PM with 0.01 mM and 0.1 mM of Ni^{2+} compared to the PM without Ni^{2+}. This indicates that trace Ni^{2+} did not significantly impair the ureolytic pathway responsible for carbonate generation.

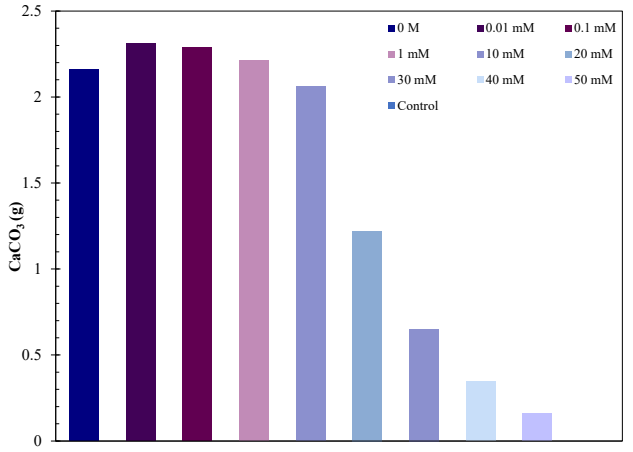

Figure 5. Amount of $CaCO_3$ precipitated in the PM at different concentrations of Ni^{2+}.

A 10 mM level of Ni^{2+} resulted in a marginal decline in the total amount of precipitation. However, when the Ni^{2+} concentration increased to 20 mM, the final $CaCO_3$ yield was reduced by ~50% relative to the PM without Ni^{2+} (Fig. 5). The precipitation rate was also slower, as evidenced by prolonged retention of soluble Ca^{2+} in the medium. This reduction is consistent with partial inhibition of urease activity.

Severe inhibition was observed at higher Ni^{2+} concentrations (30-50 mM), where precipitation yields fell below 0.6 g, even after 48 h, representing less than 30% of the maximum yield observed in the PM without Ni^{2+}. Such suppression likely stems from heavy metal toxicity disrupting cellular metabolism, impairing ammonia production and subsequent pH rise, both of which are critical for $CaCO_3$ formation (Janicka-Russak et al., 2008). Additionally, excess Ni^{2+} may interfere with crystal growth through competitive binding at nucleation sites, altering the mineralisation pathway (Magomya et al., 2017). The flat curve at the 50 mM Ni^{2+} concentration in the figure. 3 suggests not just urease inhibition, but possibly cell death, because both the precipitation rate and total yield are severely reduced. Considering the effect Ni^{2+} on the precipitation potential of *S. pasteurii*, an optimal concentration of 0.01 mM can be considered.

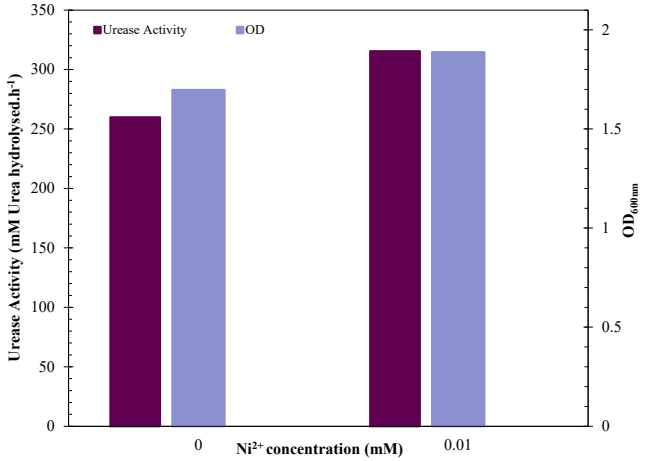

Figure 6. Maximum urease activity and biomass of S. pasteurii in the presence and absence of 0.01 mM Ni^{2+}.

The impact of 0.01 mM Ni^{2+} supplementation on the growth and ureolytic performance of *S. pasteurii* showed improvement in the biomass and enzymatic activity (Fig.6). Marginal improvement in biomass was observed with the supplementation of Ni^{2+}, whereas in the case of the enzyme activity, ~1.2-fold enhancement was observed.

These results highlight that while trace Ni^{2+} may be tolerated in cementitious MICP processes, elevated concentrations drastically diminish precipitation efficiency, posing a significant challenge for cleaner production applications in heavy metal-rich environments. Pre-treatment or adaptive acclimatisation of microbial cultures may be necessary to sustain performance in such conditions.

3.5 *Unconfined Compressive Strength (UCS)*

The treatment of the OB material with *S. pasteurii* significantly enhanced its mechanical strength. The UCS of the treated specimens exhibited an approximately eleven-fold increase compared to the untreated control. This substantial improvement can be attributed to the MICP process, wherein urease-mediated hydrolysis of urea generated carbonate ions that subsequently reacted with calcium ions to form calcite. The precipitated calcite acted as a binding agent, filling voids and coating particle surfaces, thereby increasing interparticle bonding and reducing pore space.

Table 1. UCS of OB after different days of treatment

Days	0 (untreated)	5	7	14	21
UCS (kPa)	46.6	472.8	500.91	512.6	502.6

Following bio-treatment, the UCS increased to ~470 kPa in 5days, representing an ~11-fold improvement over the control. This sharp early gain can be attributed to high bacterial activity and rapid calcite precipitation, which effectively bonded soil particles and reduced pore space.

Between days 5 and 7, UCS continued to rise modestly to ~500 kPa, indicating that the majority of precipitation and particle bonding occurred during the initial treatment phase. By day 14, UCS reached ~510 kPa, suggesting that the process had approached a plateau.

These results align with previous reports demonstrating that MICP can substantially improve the load-bearing capacity of granular or loose soils through bio-cementation (Jhuo et al., 2025; Zhang et al., 2023). The magnitude of improvement observed in this study suggests that the high urease activity of *S. pasteurii*, coupled with sufficient calcium availability, enabled extensive precipitation throughout the pore network of the OB matrix. The enhanced particle interlocking and reduced deformability contributed to the marked increase in the strength. Such improvements indicate that MICP-based stabilisation has strong potential for the valorisation of mine overburden into sustainable construction.

The influence of Ni^{2+} supplementation on the mechanical strength of bio-treated soil was evaluated by incorporating the optimised concentration of 0.01 mM Ni^{2+} into the treatment solution. It was observed that the presence or absence of this supplementation did not result in a statistically significant difference in the UCS, with both treatments yielding values in the same range (~512.6 ± 7.21 kPa). This suggests that the addition of Ni^{2+} at the tested concentration does not substantially influence the MICP process under the given experimental conditions.

One plausible explanation lies in the pre-existing heavy metal contamination of the soil. Analysis of total heavy metals revealed a nickel concentration of 13.9 mg/kg, with a leachable fraction of 0.77 mg/L. The inherent presence of Ni^{2+} in the soil may have already provided sufficient availability for bacterial urease activation, thereby rendering external supplementation redundant. From a cleaner production perspective, these findings are noteworthy. In case of soils with inherent concentrations of Ni^{2+}, care should be taken not to include additional concentrations. This not only reduces chemical inputs but also aligns sustainability goals by preventing unnecessary metal introduction, which could otherwise contribute to secondary contamination risks during field applications.

The XRD analysis revealed an additional peak at a 2θ value of 29 °C, indicating the presence of calcite (Fig. 7). The emergence of this peak, absent in the untreated control, confirms the successful precipitation of calcium carbonate through MICP. Calcite is the thermodynamically most stable polymorph of $CaCO_3$ under ambient conditions, and its presence is directly linked to the improvement in mechanical performance observed in the treated OB (Sarma and Mishra, 2024).

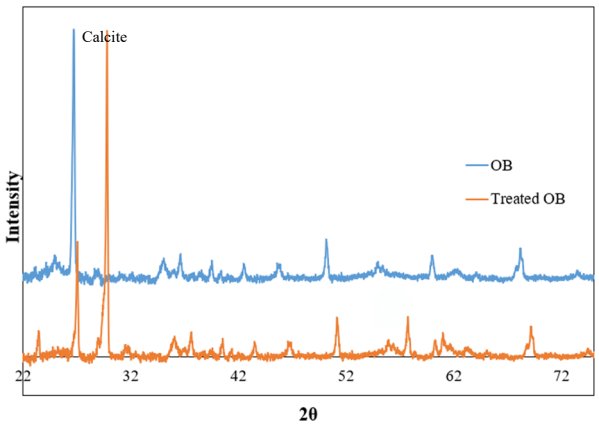

Figure 7. XRD spectrum of treated and untreated OB

4. CONCLUSION

MICP offers a sustainable and effective approach for soil stabilisation, with clear advantages over conventional methods. This study demonstrated the Ni^{2+}-dependent precipitation potential of *Sporosarcina pasteurii*, highlighting the role of Ni^{2+} as a structural cofactor essential for urease stability and activity. Low Ni^{2+} concentrations (0.01 mM) enhanced calcite formation, attributable to its role in stabilising the urease active site, while maintaining bacterial growth. The moderate concentrations of Ni^{2+} did not suppress urease function, indicating inherent metal tolerance, further underscoring its potential in treating Ni-contaminated soils without significant loss of bio-cementation capacity. MICP treatment of contaminated overburden achieved an eleven-fold increase in unconfined compressive strength within five days, demonstrating its capacity for rapid soil reinforcement. These results establish MICP as a viable cleaner production approach for advancing sustainable geotechnical engineering practices and environmentally benign technology for remediation applications.

4 ACKNOWLEDGEMENTS

The authors would like to acknowledge the BSBE department, Biopat Lab, Central Instrument Facility and Environmental Engineering Lab of IIT Guwahati for providing the facility for carrying out the experiments. The authors also thankfully acknowledge ATTC for providing the strain *S. pasteurii* ATCC11859. The authors gratefully acknowledge Ms. Sandhya S for the support in conducting the experiment.

5 REFERENCES

American Public Health Association. 1992. APHA Method 4500-NO3: Standard Methods for the Examination of Water and Wastewater.

ASTM. 1994. Standard Test Methods for Determining the Specific Gravity of Soils. D854-92. Philadelphia: American Society for Testing and Materials.

ASTM. 2010. Standard Test Methods for Determining the Unconfined Compressive Strength of Soils. D2166. Philadelphia: American Society for Testing and Materials.

ASTM. 2010. Standard Test Methods for Liquid Limit, Plastic Limit, and Plasticity Index of Soils. D 4318. Philadelphia: American Society for Testing and Materials.

ASTM. 2012. Standard Test Methods for Laboratory Compaction Characteristics of Soil Using Standard Effort. D 698. Philadelphia: American Society for Testing and Materials.

ASTM. 2017. Standard Test Methods for Determining the Amount of Material Finer than 75-µm (No. 200) Sieve in Soils by Washing.

D 1140. Philadelphia: American Society for Testing and Materials.
Carter, M.S., Tuttle, M.J., Mancini, J.A., Martineau, R., Hung, C.-S., Gupta, M.K., 2023. Microbially Induced Calcium Carbonate Precipitation by Sporosarcina pasteurii: a Case Study in Optimizing Biological CaCO3 Precipitation. Applied and Environmental Microbiology 89, e01794-22. https://doi.org/10.1128/aem.01794-22
Cui, H., Wang, Z., Ye, B., Hu, K., Xu, P., Zhou, Jing, Ge, L., Zheng, X., Zhou, Jun, 2023. Comprehensive evaluation on safe utilization potential of ten oilseed rape cultivars in a cadmium contaminated soil. Environmental Technology & Innovation 32, 103329. https://doi.org/10.1016/j.eti.2023.103329
El-Naggar, A., Ahmed, N., Mosa, A., Niazi, N.K., Yousaf, B., Sharma, A., Sarkar, B., Cai, Y., Chang, S.X., 2021. Nickel in soil and water: Sources, biogeochemistry, and remediation using biochar. Journal of Hazardous Materials 419, 126421. https://doi.org/10.1016/j.jhazmat.2021.126421
EPA, E. P., 1992. Method 1311: Toxicity characteristic leaching procedure. US Environmental Protection Agency.
Fopase, R., Nayak, S., Mohanta, M., Kale, P., Paramasivan, B., 2019. Inhibition assays of free and immobilized urease for detecting hexavalent chromium in water samples. 3 Biotech 9, 124. https://doi.org/10.1007/s13205-019-1661-4
Fouladi, A.S., Arulrajah, A., Chu, J., Horpibulsuk, S., 2023. Application of Microbially Induced Calcite Precipitation (MICP) technology in construction materials: A comprehensive review of waste stream contributions. Construction and Building Materials 388, 131546. https://doi.org/10.1016/j.conbuildmat.2023.131546
Fu, T., Saracho, A.C., Haigh, S.K., 2023. Microbially induced carbonate precipitation (MICP) for soil strengthening: A comprehensive review. Biogeotechnics 1, 100002. https://doi.org/10.1016/j.bgtech.2023.100002
Ge, R.-G., Wang, D.-X., Hao, M.-C., Sun, X.-S., 2013. Nickel trafficking system responsible for urease maturation in Helicobacter pylori. World Journal of Gastroenterology 19, 8211–8218. https://doi.org/10.3748/wjg.v19.i45.8211
Giannis, A., Pentari, D., Wang, J.-Y., Gidarakos, E., 2010. Application of sequential extraction analysis to electrokinetic remediation of cadmium, nickel and zinc from contaminated soils. Journal of Hazardous Materials 184, 547–554. https://doi.org/10.1016/j.jhazmat.2010.08.070
Janicka-Russak, M., Kabała, K., Burzyński, M., Kłobus, G., 2008. Response of plasma membrane H+-ATPase to heavy metal stress in Cucumis sativus roots. J Exp Bot 59, 3721–3728. https://doi.org/10.1093/jxb/ern219
Jhuo, Y.-S., Wong, H.-E., Tung, H.-H., Ge, L., 2025. Effectiveness of microbial induced carbonate precipitation treatment strategies for sand. Environmental Technology & Innovation 38, 104132. https://doi.org/10.1016/j.eti.2025.104132
Magomya, A.M, J.T, B., S.A, O., 2017. Assessment of Metal - Induced Inhibition of Soybean Urease as a Tool for Measuring Heavy Metals in Aqueous Samples. IOSR JAC 10, 61–70. https://doi.org/10.9790/5736-1006026170
Mi, T., Peng, L., Yu, K., Zhao, Y., 2023. Enhancement strategies for recycled brick aggregate concrete using MICP and EICP treatments. Journal of Building Engineering 79, 107909. https://doi.org/10.1016/j.jobe.2023.107909
Rajasekar, A., Zhao, C., Wu, S., Murava, R.T., Norgbey, E., Omoregie, A.I., Moy, C.K.S., 2025. Removal of high concentrations of zinc, cadmium, and nickel heavy metals by Bacillus and Comamonas through microbially induced carbonate precipitation. Biodegradation 36, 40. https://doi.org/10.1007/s10532-025-10131-7
Sarma, S., Mishra, A.K., 2024. Microbial-Induced Calcium Carbonate Precipitation – A Potentially Sustainable Approach for Geo-environmental Challenges: A Retrospection into the Mechanism, Influencing Factors, Characterization, and Applications. Geomicrobiology Journal 41, 921–938. https://doi.org/10.1080/01490451.2024.2401887
Sarma, S., S, S., Mishra, A.K., 2025. Leveraging a Tailor-Made Approach to Enhance the Kinetics of a Native Ureolytic Bacterium, Sporosarcina Pasteurii Ps3a, for Effective Bio-Cementation. https://doi.org/10.2139/ssrn.5258809
Yang, Z., Liu, L., Dong, Y., Gao, Z., 2024. Comparative study on the effect of SRB and Sporosarcina pasteurii on the MICP cementation and solidification of lead–zinc tailings. Chemical Engineering Journal 495, 153446. https://doi.org/10.1016/j.cej.2024.153446
Yin, J., Wu, J.-X., Zhang, K., Shahin, M.A., Cheng, L., 2023. Comparison between MICP-Based Bio-Cementation Versus Traditional Portland Cementation for Oil-Contaminated Soil Stabilisation. Sustainability 15, 434. https://doi.org/10.3390/su15010434
Zhang, Q., Ye, W., Liu, Z., Wang, Q., Chen, Y., 2023. Influence of injection methods on calcareous sand cementation by EICP technique. Construction and Building Materials 363, 129724. https://doi.org/10.1016/j.conbuildmat.2022.129724